

# **Molecular orientation for vapor-deposited organic glasses follows rate-temperature superposition: The case of posaconazole**

Authors: Camille Bishop<sup>1</sup>, Yuhui Li<sup>2</sup>, Michael F. Toney<sup>3</sup>, Lian Yu<sup>1,2</sup>, M.D. Ediger<sup>\*,1</sup>

1. University of Wisconsin – Madison, Department of Chemistry. 1101 University Ave, Madison, WI 53706.
2. University of Wisconsin – Madison, School of Pharmacy. 777 Highland Ave, Madison, WI 53705.
3. SLAC National Accelerator Laboratory. 2575 Sand Hill Rd, Menlo Park, CA 94025.

\*Corresponding author email: [ediger@chem.wisc.edu](mailto:ediger@chem.wisc.edu). Phone: 608-262-7273

## Abstract

The anisotropic properties of organic glasses produced by physical vapor deposition (PVD) depend upon substrate temperature and deposition rate. In recent work, it was shown for a liquid crystalline system that the anisotropic structure of the glass was controlled by a single combined variable as indicated by the observation of Deposition Rate-Substrate Temperature Superposition (RTS). Here we test the utility of RTS for posaconazole, a molecule that does not form liquid crystals. We prepare glasses of posaconazole utilizing a range of deposition rates covering two orders of magnitude and an 18 K range in substrate temperature. We characterize the glasses using ellipsometry and X-ray scattering. Consistent with RTS, we find that decreasing the deposition rate has the same effect upon molecular orientation as increasing the substrate temperature during deposition. Thus RTS can be used to predict and control the structure of glasses prepared at a wide range of deposition conditions. We use RTS to infer a characteristic time for molecular reorientation at the surface of posaconazole.

## Introduction

Thin glassy films are a vital component in many current technologies. Many classes of materials can be made amorphous, including inorganic metal alloys,<sup>1</sup> chalcogenides,<sup>2</sup> and oxides;<sup>3</sup> and organic polymer<sup>4</sup> and molecular<sup>5</sup> systems. Currently, organic glassy films are incorporated in and being developed for thin film organic electronic applications such as light-emitting diodes (OLEDs),<sup>6-9</sup> photovoltaics,<sup>10</sup> and transistors.<sup>11</sup> Because glasses are out-of-

equilibrium, they can be prepared in a variety of physical states to optimize their properties. Physical vapor deposition (PVD) is one way to tailor the properties of glasses for specific applications. Compared to glasses prepared by liquid cooling, glasses produced by PVD have exceptional properties such as anisotropic molecular organization,<sup>12-14</sup> and higher kinetic stability<sup>15-19</sup> and density.<sup>20-21</sup> The deposition conditions used in PVD have been shown to have an important influence on OLED performance.<sup>9</sup>

The properties of glasses produced by PVD can be understood by a surface equilibration mechanism.<sup>12-13, 22</sup> During deposition, enhanced mobility<sup>23</sup> at the free surface of a glass allows the newly deposited molecules to partially (or fully) equilibrate toward structures favored at the surface before becoming trapped by further deposition. In this way, a bulk glass is built up with structural properties that would generally exist only within a few nanometers of the free surface.<sup>24</sup> Since molecular packing at the free surface is anisotropic, this often results in highly ordered glasses. For example, in itraconazole, recent results suggest that the end-over-end motion of the rod-like molecules, which has been studied in the bulk,<sup>25-26</sup> is kinetically arrested by further deposition after partial equilibration at the free surface, resulting in molecular order characteristic of a smectic liquid crystal.<sup>27</sup> As to the question which measure of surface mobility (translational diffusion, molecular rotation, or others) best describes the surface equilibration process relevant for the properties of PVD glasses, previous work has emphasized surface diffusion simply because more data of the sort were available and has shown that systems with faster surface diffusion generally form more stable glasses.<sup>23, 28-30</sup> Recent studies have pointed to a need to consider other types of surface mobility responsible for distinct properties of vapor-deposited glasses.<sup>27, 31-33</sup>

Recently, it has been found that the effects of deposition rate and substrate temperature upon the structure of a vapor-deposited glass can be related by a “Deposition Rate-Substrate Temperature Superposition” (RTS).<sup>27</sup> This RTS principle can be understood from the perspective of the surface equilibration mechanism, as raising the substrate temperature (at fixed deposition rate) and decreasing the deposition rate (at fixed substrate temperature) both give the molecules greater opportunity for equilibration. A property of a vapor-deposited glass is said to obey RTS if, from a change in the substrate temperature that modifies the property by a certain amount, one can predict the change in deposition rate required to modify the property by the same amount.

The principle of RTS may be thought of as analogous to time-temperature superposition<sup>34-35</sup> or isochronal superposition<sup>36</sup> in describing the dynamics of glasses and supercooled liquids, in which external variables such as temperature and pressure shift the timescale of relaxations without changing the relaxation mechanism.

So far, RTS has been demonstrated for itraconazole, a molecule with smectic liquid crystal phases. One advantage of using itraconazole to investigate RTS is that highly anisotropic structural features, including both orientational and translational order, allow one to observe large changes in structure from relatively small changes in deposition conditions. For itraconazole, reducing the deposition rate by 60% at a fixed temperature has the same effect on molecular orientation as increasing the substrate temperature by 1 K. RTS allowed the identification of distinct relaxation processes at the surface, and connected them to the final structure of the as-deposited glass.<sup>27</sup> The utility of RTS is two-fold: it can be used both to study the processes at the free surface of the glass, and also to predict the structure of glasses deposited over a wide range of conditions. As many systems used for organic electronics do not have equilibrium liquid crystal phases, it is of interest to test RTS in a system that does not form liquid crystals, to more generally determine its utility for controlling anisotropic structure in glasses.

In this work, we investigate posaconazole, a molecule without any known equilibrium liquid crystal phases, and show that the molecular orientation of its vapor-deposited glasses can be described by RTS. Posaconazole has a high degree of anisotropy when prepared by PVD,<sup>37</sup> making it a good candidate for unambiguous determination of the effects of both rate and substrate temperature upon glass structure. We vapor deposited posaconazole at many rates and substrate temperatures above  $0.94T_g$  and investigated the structure of the resulting glasses using ellipsometry and X-ray scattering. We show that molecular orientation in PVD glasses of posaconazole obeys RTS, and we use the results to infer rates of molecular orientational mobility at the free surface of the glass.

## Methods

### *Vapor Deposition of Films*

Posaconazole VETRANAL analytical standard was used as-received from Sigma Aldrich. Glasses were deposited on Si <1 0 0> wafers with a native oxide surface layer (Virginia Semiconductor). A custom-built vacuum chamber with substrate temperature control was used, with a source-to-substrate distance of 11 cm, as detailed in previous publications.<sup>37-38</sup> The deposition rate was monitored using a quartz crystal microbalance (Sycon) to ensure a constant rate. Deposition rates reported in this work are determined by the ellipsometrically-determined film thickness divided by the total deposition time. Posaconazole glasses were deposited over a range of substrate temperatures and deposition rates. Films utilized for birefringence and GIWAXS measurements were between 200 and 1000 nm thick. Previous work has established that film structure is independent of film thickness in the range 100 – 1000 nm.<sup>13, 38</sup>

#### *Characterization of as-deposited films*

Spectroscopic Ellipsometry (SE) measurements were made using a J.A. Woollam M-2000U ellipsometer. Measurements were made at 7 angles at 21 points on each 1-inch wafer. The data in the wavelength range from 500-1000 nm was analyzed using an anisotropic Cauchy model, in which

$$n_o = A_o + \frac{B}{\lambda^2}, n_e = A_e + \frac{B}{\lambda^2}$$

Here  $n_o$  is the refractive index in the plane of the film and  $n_e$  is the refractive index out of the plane. Because of the short source-to-substrate distance, film thicknesses on a given wafer vary by as much as 50%, creating a range of deposition rates that we utilize in our analysis.

Birefringence data shown below for posaconazole are from individual measurements (spot size ~0.6 mm x 1.5 mm) and not averaged. Thus, from one sample, 21 deposition rates and birefringence values are reported.

Grazing incidence wide-angle X-ray scattering (GIWAXS) was performed at beamline 11-3 of the Stanford Synchrotron Radiation Lightsource (SSRL). The sample-to-detector distance was 300 mm, and the X-ray energy was 12.7 keV. Grazing-incidence patterns used in this work were taken at  $\theta_{in} = 0.14^\circ$  with an exposure time of 120 s. Near-specular exposures were taken for  $q \sim 0.2$  and  $0.4 \text{ \AA}^{-1}$  peaks to confirm the absence of sharp peaks directly along  $q_z$ ;<sup>39</sup> in light of the low signal-to-noise ratio, we do not present quantitative analysis of these exposures. The two-dimensional patterns are presented in SI section 1.

GIWAXS data was analyzed using the WAXSTools plugin<sup>40</sup> in the Nika software package<sup>41-42</sup> for Igor, which corrects for the “missing wedge” due to the geometry of grazing incidence. 1-dimensional integrations shown below in Figure 3B are the sum of all integrated intensity between  $\chi = 4^\circ$  to  $8^\circ$  and  $-4^\circ$  to  $-8^\circ$ ; here  $\chi$  is the polar angle from the surface normal. Intensities are corrected for sample thickness, with an empirical B-spline background subtracted.

### *Determination of $T_g$*

To allow a careful comparison of glass formation in posaconazole and itraconazole, we performed differential scanning calorimetry (DSC) experiments to determine the glass transition temperature  $T_g$  for each system. Samples of each liquid were cooled at 10 K/min and then heated at 10 K/min, with  $T_g$  determined as the onset temperature upon heating.  $T_g$  values of 331 K for posaconazole and 328 K for itraconazole were obtained. These results agree with literature values within 2 K.<sup>25, 38, 43-44</sup>

### Results

Posaconazole (structure shown in Figure 1A) was vapor deposited at substrate temperatures ranging from 310 K to 328 K ( $0.94$  to  $0.99T_g$ ) and deposition rates from  $0.1$  to  $10 \text{ \AA s}^{-1}$ . The optical birefringence of these glasses, which is proportional to the molecular orientation order parameter  $S_z$  to a good approximation,<sup>45</sup> was measured by spectroscopic ellipsometry. Figure 2A shows the birefringence of the as-deposited posaconazole as a function of deposition rate for several substrate temperatures. For one of the lower substrate temperatures, 315 K, depositing at the highest rate results in a birefringence of  $-0.02$ , indicating a tendency towards horizontal orientation. At the same substrate temperature, when the rate is decreased by a factor of 15, the birefringence of the resulting glass is  $0.04$ , indicating more vertically oriented molecules. At the highest substrate temperatures, the birefringence is not monotonic with respect to changes in the deposition rate. For example, the glass prepared at 328 K at the fastest rate has a birefringence of  $0.10$ . When the deposition rate is decreased, the birefringence first increases to  $0.12$  and then decreases to  $0.03$ .

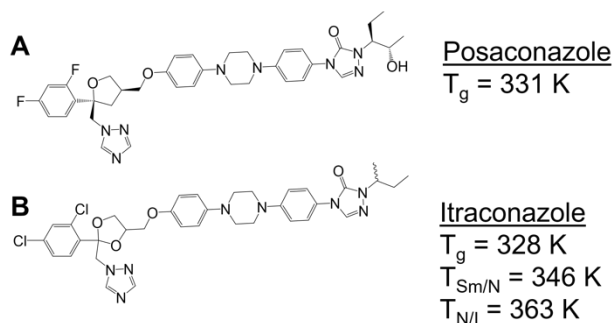


Figure 1. The molecular structures and thermal transitions<sup>38</sup> of A) posaconazole and B) its structural analog, itraconazole.

While it may appear that the deposition rate data in Figure 2A does not follow any systematic trend, deposition rate-substrate temperature superposition (RTS) can be used to reveal an underlying pattern. By horizontally shifting all birefringence vs. deposition rate data, the curves approximately collapse into a single “master curve”. It is significant that the master curve can be obtained with a single “shift factor”, 0.22 decade per K. The shift factor was obtained using a fitting procedure for the entire data set (see SI Section 2). Figure 2B uses this shift factor to construct the superposition of data from Figure 2A. In Figure 2B, the x-values for the data are presented as an “effective deposition rate” which is calculated using this shift factor. The effective deposition rate is the rate (according to RTS) that would be necessary to produce a glass with a given birefringence at the specified reference substrate temperature (328 K). For example, RTS predicts that the birefringence of a sample prepared at  $2 \text{ \AA s}^{-1}$  at 320 K (8 K below the reference temperature) could be matched at a substrate temperature of 328 K if the deposition rate were increased by 1.76 decades (to  $115 \text{ \AA s}^{-1}$ ). The best fit value of the shift factor ( $0.22 \text{ decades K}^{-1}$ ) signifies that raising the substrate temperature by 1 K has the same effect upon molecular orientation as depositing 1.7 times more slowly. Also shown in Figure 2B is previously published data on PVD glasses of itraconazole by Gómez et. al.,<sup>38</sup> in these experiments, a single deposition rate ( $2 \text{ \AA s}^{-1}$ ) and many substrate temperatures were utilized. Good agreement is observed between our new results and the previously published data.

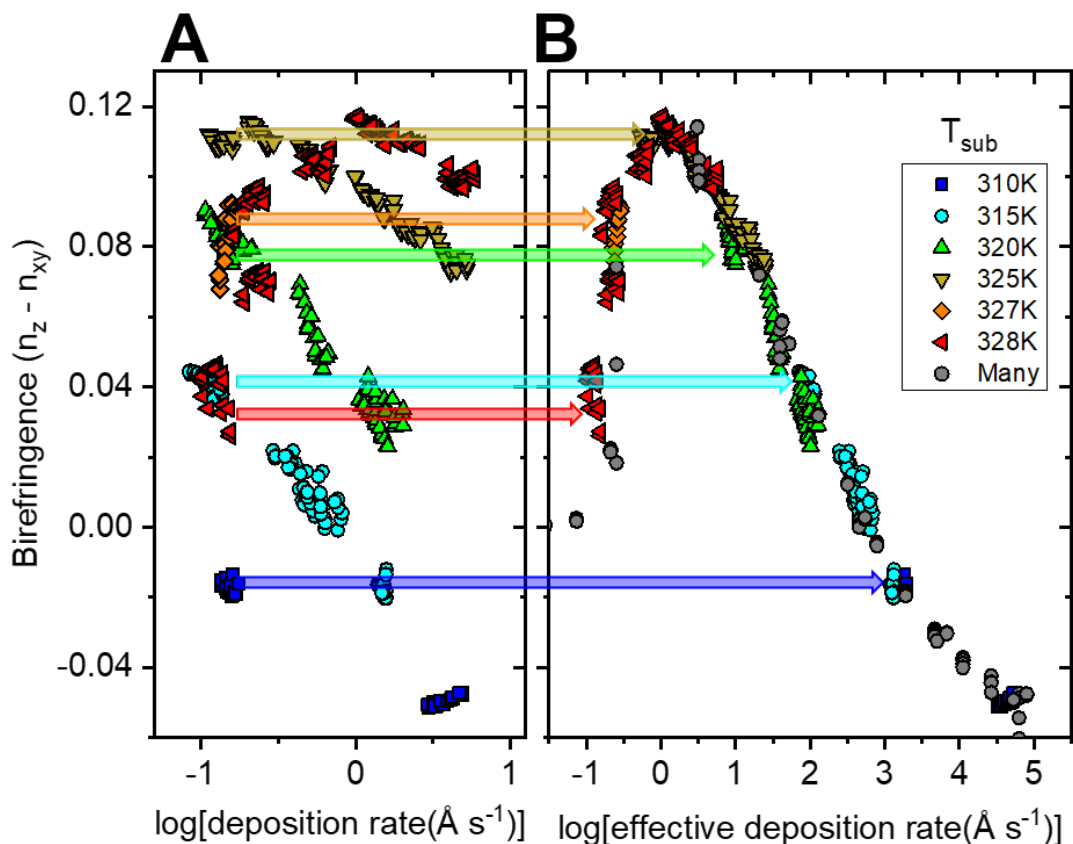


Figure 2. The molecular orientation of posaconazole obeys deposition rate-temperature superposition (RTS). A) Birefringence of vapor-deposited posaconazole at several substrate temperatures as a function of the log of deposition rate. B) Birefringence data shown in panel A, shifted to an “effective deposition rate at 328K” by applying a shift factor of 0.22 decades in deposition rate per K in substrate temperature. Gray data is from J. Gómez et. al.<sup>38</sup> (deposited at a rate of  $2 \text{ \AA s}^{-1}$  at many different substrate temperatures), shifted by the factor found in this work.

GIWAXS measurements allow the characterization of translational ordering in PVD glasses of posaconazole and, in combination with the birefringence measurements, allow insights into the surface structure of posaconazole. Figure 3 shows the two-dimensional grazing-incidence wide-angle X-ray scattering (GIWAXS) of two glasses with the same birefringence but different effective deposition rates. The two-dimensional scattering patterns are shown in Figure 3A, and the integrated scattering along  $q_z$  is shown in Figure 3B. (More information about specific integration limits is provided in *Methods*.) Both glasses have scattering peaks at  $q \sim 0.2$ ,

0.45, and  $0.7 \text{ \AA}^{-1}$ , which correspond to translational smectic-like ordering in the glass.<sup>14</sup> While the peak at  $q \sim 0.2 \text{ \AA}^{-1}$  appears to differ between the two glasses, the close proximity to the beamstop partially obscures the feature, making a quantitative analysis difficult. Therefore, we focus our analysis on the peaks at  $q \sim 0.45$  and  $0.7 \text{ \AA}^{-1}$ . These scattering peaks indicative of translational smectic-like order are significantly weaker in the glass deposited at the lower effective rate, even though these two glasses have similar molecular orientation. We return to this observation in the discussion below.

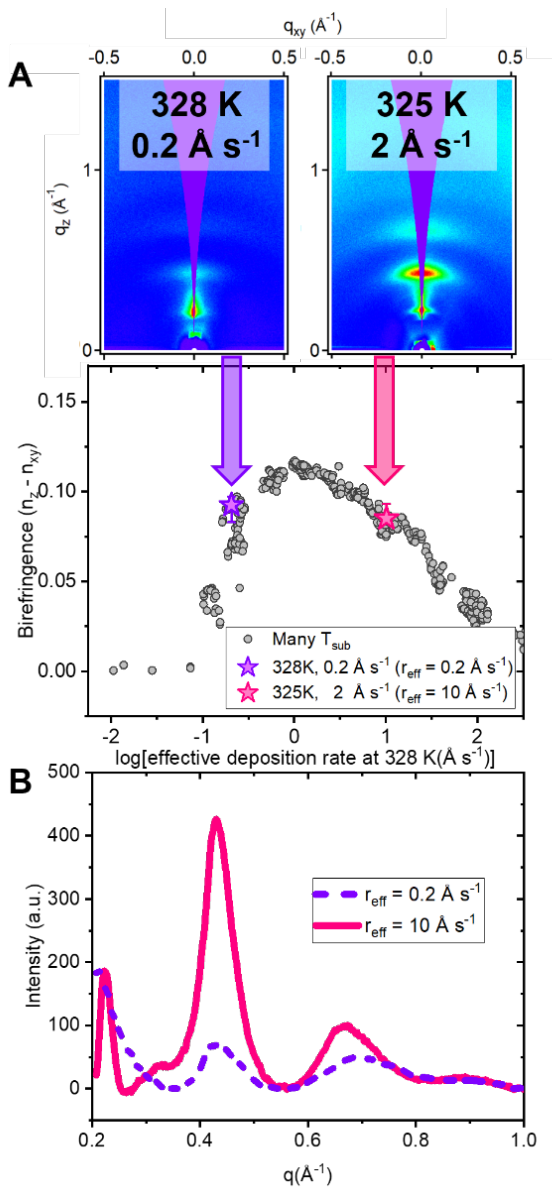




Figure 3. X-ray scattering reveals decreased structural order in glasses prepared at lower effective deposition rates even though the two glasses have similar levels of average molecular orientation. Experiments are performed using an incident angle  $\theta_{in}$  of  $0.14^\circ$ , which is greater than the critical angle for posaconazole, to probe the structure of the entire film. A) 2-dimensional grazing-incidence wide-angle X-ray scattering patterns of two glasses with the same birefringence. One glass is prepared at low effective rate, and the other at a higher effective rate. Bars on birefringence vs. effective rate plot denote the minimum and maximum birefringence of the sample measured. B) Out-of-plane X-ray scattering near  $q_z$  as a function of  $q$  for the patterns shown in A. The glass deposited at the lower effective rate has less translational order as indicated by the diminished scattering intensity.

## Discussion

### *Near-surface structure of posaconazole.*

We can utilize the data in Figures 2 and 3, together with additional experimental information, to produce a qualitative picture of the surface structure of the supercooled liquid of posaconazole, as shown in Figure 4A. Previously performed NEXAFS<sup>37</sup> experiments show that molecules in the top ~6 nm of the equilibrium surface are, on average, vertically oriented. Ellipsometry shows that the bulk liquid is isotropic. Other features of Figure 4A, particularly the loss of orientational and translational order as distance from the interface increases, are inferences from vapor deposition experiments, as we discuss next.

Our construction of Figure 4A draws upon previous simulations<sup>46</sup> that concluded that the structure of a vapor-deposited glass is determined by the depth of equilibration during deposition. Molecular dynamics simulations by Lyubimov et. al., performed for the rod-like organic electronics molecule TPD, modeled both the vapor deposition of the glass and the equilibrium surface structure of the liquid. The final molecular orientation of the vapor-deposited glass was found to match the molecular orientation at a depth in the equilibrium liquid which depended upon both the substrate temperature and the deposition rate.<sup>46</sup> In Figure 4A, we have indicated approximate equilibration depths during deposition at different effective rates with colored regions, as discussed below.

We first discuss the features of the birefringence master curve (Figure 2B and Figure 4B) in light of the schematic in Figure 4A. At very high effective rates, the birefringence is quite negative, consistent with predominantly in-plane orientation of the long axes of the posaconazole molecules. In this regime, we expect that there is so little time on the surface that incoming molecules lie flat to minimize their energy, even though molecules at the surface would be vertically oriented at equilibrium. At an effective deposition rate of  $10 \text{ \AA s}^{-1}$ , glasses with positive birefringence (vertical orientation) are formed. For such a deposition, molecules at the surface have almost enough time to completely equilibrate to the strong vertical orientation shown for the equilibrium liquid before being trapped by additional deposition. Thus the glass nearly achieves the maximum possible orientation, which is formed when more time is available for equilibration (corresponding to an effective rate of  $1 \text{ \AA s}^{-1}$ ). At an effective deposition rate of  $0.2 \text{ \AA s}^{-1}$ , equilibration extends well into the second layer. Further deposition traps the orientation of this region away from the surface and thus the overall glass structure does not quite achieve the maximum possible orientation. Finally, at an effective deposition rate of  $0.004 \text{ \AA s}^{-1}$ , equilibration extends far enough from the free surface that the structure is isotropic; further deposition traps this isotropic orientation into the bulk glass which, as a result, has zero birefringence. In general, there is the possibility of an additional mechanism influencing the measured birefringence, such that molecular orientation decays due to a bulk process during long depositions. For posaconazole, we find that this is a small effect. For example, at  $T_{\text{sub}} = 327 \text{ K}$ , we estimate that the measured birefringence has decayed  $\sim 13\%$  due to bulk relaxation. At lower values of  $T_{\text{sub}}$ , the impact of this bulk process will be even smaller (see SI section 3 for further discussion).

The GIWAXS results in Figure 3 provide evidence that the tendency for layering near the free surface of posaconazole is quickly lost as the distance from the interface increases. In particular, we interpret the strong smectic layering observed at an effective deposition rate of  $10 \text{ \AA s}^{-1}$  to indicate that partial equilibration towards the structure of the top monolayer includes substantial layering. In contrast, the weak layering observed in the glass at an effective deposition rate of  $0.2 \text{ \AA s}^{-1}$  indicates that the equilibrium structure below the top monolayer does not show much smectic order. While the equilibration distances shown in Figure 4A are speculative, we expect that this conclusion is robust: orientational order persists further from than interface than does translational order.

This work shows that it is possible to use vapor deposition as a tool (qualitative, at this point) to study the structure of liquid surfaces. The advantage of vapor deposition in this respect is that it is much easier to study the bulk structure of a thin film (using, for example, ellipsometry and GIWAXS) than to selectively characterize the top few nm near the surface. Vapor deposition traps the surface structure into a bulk material where it can be examined with many standard techniques.

Previous characterizations of surface mobility in small molecule<sup>32</sup> and polymer<sup>47</sup> glasses typically estimate the mobile layer to be ca. 5 nm near  $T_g$ , consistent with the length scales of the mechanism proposed here. For an absolute experimental determination of the equilibration depth at various effective rates, the depth-dependent orientational and translational order must be resolved. While we do not yet know this structure for posaconazole, emerging polarized resonant soft X-ray reflectivity (p-RSoXR) techniques may be useful in the future for a quantitative understanding.<sup>48</sup>

#### *Near-surface dynamics of posaconazole.*

We can use the comparison of molecular orientation in posaconazole and itraconazole glasses to find the relative timescales of surface reorientation for the two systems, and show that surface reorientation is approximately 1.5 orders of magnitude slower for posaconazole. Previous work on itraconazole suggests that the rate of end-over-end molecular reorientation determines orientational order in the bulk,<sup>25-26</sup> and that this reorientation process near the free surface determines the molecular orientation (birefringence) trapped into the PVD glass.<sup>27</sup> For itraconazole, a more birefringent glass results when more reorientation occurs at the free surface during deposition. In Figure 4B, the birefringence for glasses of itraconazole and posaconazole are compared, with both systems shifted to a common reference temperature of 328 K. For both systems, at high effective deposition rates, the molecules do not have enough time and/or mobility to partially equilibrate during deposition, so they remain trapped in their initial (horizontal) orientation for both systems. As the effective rate is lowered, the birefringence of itraconazole increases first, indicating a faster surface reorientation process. At intermediate effective rates, where both systems are equilibrating toward a vertically oriented surface layer, an effective rate of  $10^{1.7} \text{ \AA s}^{-1}$  results in a birefringence of 0.044 for posaconazole. The effective rate required to deposit an itraconazole glass with the same birefringence of 0.044 is  $10^{3.0} \text{ \AA s}^{-1}$ . Thus,

we infer that at 328 K, surface reorientation is about 20 times faster for itraconazole than for posaconazole. As only the surface structures of itraconazole and posaconazole are similar, the two systems can only be fairly compared at effective rates above  $10 \text{ \AA s}^{-1}$ , in which the structure of the equilibrating region is mostly vertically oriented for both systems.

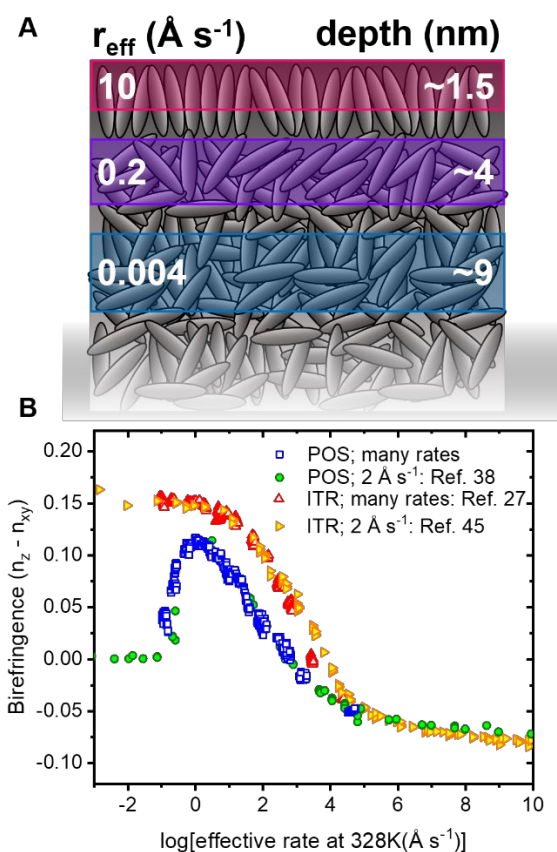


Figure 4. The depth of equilibration, which depends on the effective deposition rate, explains the decrease in order of vapor-deposited posaconazole at low effective rates. A) Illustration of the proposed equilibrium surface structure of posaconazole, and the equilibration depth at various rates at 328 K. Colors are chosen to illustrate equilibration depths for the cases shown in Figure 3. B) The birefringence for posaconazole (shown in Figure 2B) and itraconazole compared side-

by-side. At effective deposition rates greater than  $0.2 \text{ \AA s}^{-1}$ , the birefringence of posaconazole is less than that of itraconazole, consistent with slower surface relaxation in posaconazole.

For our continuing discussion, it is useful to compare the bulk and surface relaxation times for posaconazole and itraconazole, as shown in Figure 5. Bulk  $\tau$  values from previous dielectric and modulated DSC studies<sup>25, 44</sup> are shown for both itraconazole and posaconazole. For posaconazole, we have added previously measured relaxation times for the bulk birefringence (pink stars) to the dielectric data as these should characterize the same process;<sup>38</sup> see SI section 3 for additional details. Previously determined surface  $\tau$  values for itraconazole are also plotted in Figure 5, and show several orders of magnitude enhancement relative to the bulk  $\tau$  values for itraconazole. The solid line representing the temperature dependence of the posaconazole surface relaxations as determined by the RTS shift factor (Figure 2), and the horizontal shift between the two systems from Figure 4B determines its position relative to the solid line representing itraconazole.

Also in Figure 5, we plot independently determined surface relaxation times ( $\tau_{\text{surf}}$ ) for posaconazole (pink closed triangles), obtained using Kohlrausch-Williams-Watts (KWW) fitting as detailed in SI Section 4. For these fits, the birefringence of vapor-deposited glasses is plotted versus a surface residence time, which is determined assuming a 3 nm mobile layer, corresponding to the length of one molecule. The data is fit to a KWW function of the form

$$\Delta n = A * \exp\left(-\left(t/\tau_{\text{surf}}\right)^\beta\right) + C \quad (1)$$

with C equal to the birefringence corresponding to the equilibrium surface orientation at the deposition temperature, A+C equal to the birefringence corresponding to the initial orientation of the molecules when they first add to the growing film, and  $\beta$  a stretching exponent. The  $\tau_{\text{surf}}$  determined by this method is a measure of how long it takes for a molecule in the surface layer to reorient from initially horizontal to the (mostly vertical) equilibrium surface orientation. The same procedure was previously used to determine the surface reorientation time for itraconazole by Bishop et. al.<sup>27</sup> Consistent with the analysis performed above using Figure 4B, we note that the KWW fitting procedure shows that surface reorientation is approximately 1.5 orders of magnitude slower for posaconazole than for itraconazole at the same temperature. As an

alternate procedure, one could shift the temperature scale in Figure 5 to force the bulk  $\tau$  values to superpose; this shift is approximately 3 K and would reduce the difference between posaconazole and itraconazole.

Figure 5 shows that, near  $T_g$  (at 330 K), the surface reorientation time for posaconazole is approximately 3.5 orders of magnitude faster than the bulk process, which is consistent with the surface equilibration mechanism discussed above. The  $\tau_{\text{bulk}}$  at 330 K found here is  $10^{3.1}$  seconds compared to the extrapolated  $\tau_{\text{surf}}$  of  $10^{-0.6}$  seconds. In order for the surface equilibration mechanism to be effective, the mobility must be enhanced at the surface relative to the bulk, as this analysis confirms.

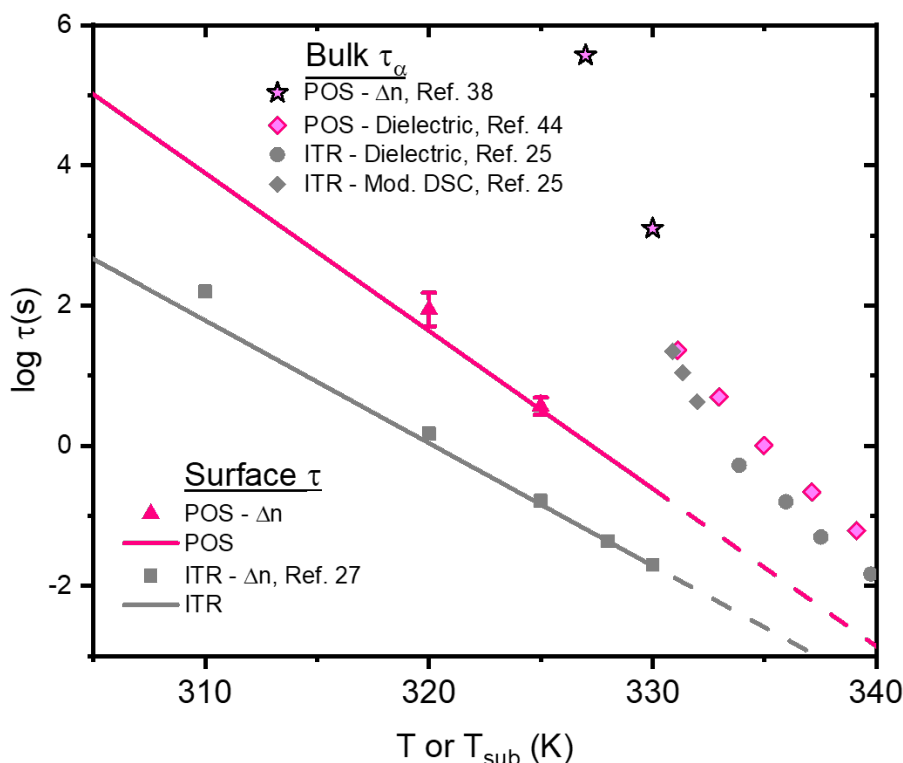


Figure 5. Times for the surface and bulk relaxations of posaconazole (POS) and itraconazole (ITR). Bulk relaxation times are from dielectric and modulated DSC measurements by Adrjanowicz et. al.<sup>44</sup> and Tarnacka et. al.,<sup>25</sup> as well as fit from birefringence annealing studies of J. Gómez et. al.<sup>38</sup> The slopes and intercepts of the POS and ITR  $\tau_{\text{surf}}$  lines are found from shift factors, as described in text. KWW fitting (shown in SI section 4) on birefringence data shown in

Figure 1A yields the two POS relaxation times shown at 320 K and 325 K, the same method that was used for ITR in a previous publication.<sup>27</sup>

The slower surface reorientation of posaconazole relative to itraconazole, as shown in Figure 5, needs to be considered in light of information from previous vapor deposition studies of the two molecules. It has been shown that, under comparable deposition conditions, PVD glasses of posaconazole have higher kinetic stability than those of itraconazole.<sup>38</sup> This is surprising as higher kinetic stability implies faster surface relaxation processes, which is opposite to the result shown in Figure 5. We think that the key to understanding this result is the existence of multiple relaxation processes at the surface of organic glasses. In earlier work, surface diffusion was used as the measure of surface mobility simply because no other data were available. For many systems, there is a good correlation between surface diffusion coefficients and the kinetic stability of PVD glasses.<sup>23,28</sup> However, a number of recent observations do not support the view that surface diffusion always controls the properties of PVD glasses. For example, recent work by Samanta et. al.<sup>31</sup> found that a system with very small surface diffusion coefficients forms a glass with high kinetic stability when vapor deposited. Laventure et. al.<sup>28</sup> noted that, for some systems, PVD glasses which did not show kinetic stability showed other properties commonly found in highly stable glasses, such as enhanced density; this result could be interpreted as indicating that one type of surface mobility is relevant for enhanced density while some other type of surface mobility controls kinetic stability. Recent work by Bishop et al.<sup>27</sup> showed that RTS applied both to molecular orientation and the spacing of smectic layers in PVD glasses of itraconazole. However, the different shift factors for these two processes implies that different surface relaxation processes (with distinct temperature dependences) are relevant for the two observables. Theoretical work on films of *n*-octane films shows that there is a significant decoupling between orientational and translational dynamics in the structured monolayer that forms at the free surface,<sup>49</sup> and this may provide a starting point for further investigation. It is possible that for PVD glasses of itraconazole and posaconazole, orientational motions at the surface control molecular orientation in the glass while the smectic structure is controlled by translational motion at the surface.

Taken together with previous studies, our present work supports the view that multiple measures of surface mobility must be considered when predicting the properties of vapor-deposited glasses. Moving forward, it may be useful to consider a combined approach utilizing simulations of surface reorientation during deposition<sup>33, 46</sup> and experimental techniques that have previously been used for polymer glass surfaces, such as Brillouin light scattering,<sup>50</sup> probe reorientation measurements,<sup>51</sup> and monitoring surface orientation evolution of a perturbed surface using NEXAFS.<sup>52</sup>

#### *Generality of Rate-Temperature Superposition.*

RTS is a useful tool that can be used to correlate and predict the structure of glasses prepared over a wide range of deposition conditions. For systems which obey RTS, the deposition conditions can be adjusted to produce the desired structure while best matching material availability, energy efficiency, and other engineering or manufacturing constraints. Through the surface equilibration mechanism, RTS can be understood as the consequence of equilibration during deposition on a particular observable; increased equilibration that results from increased temperature or decreased deposition rate should have equivalent effects. As long as the equilibrium liquid surface structure does not change appreciably over the substrate temperature range of interest (and assuming that bulk relaxation during deposition can be ignored), RTS should hold. For posaconazole the equilibrium liquid surface structure is only known near  $T_g$ <sup>37</sup>; since RTS holds, we infer that the equilibrium surface structure is similar over the range of deposition temperatures.

The work undertaken here shows that the RTS principle can be extended to systems that do not have equilibrium liquid crystal phases. RTS<sup>27</sup> was previously shown to be valid for itraconazole, posaconazole's structural analog that has equilibrium liquid crystal phases directly above  $T_g$ . Posaconazole, unlike itraconazole, is an isotropic liquid above  $T_g$ , and thus liquid crystal phases are not required for a system to obey an RTS principle. The shift factors for the two systems are similar, but not identical. The shift factor for itraconazole is 0.18 decades  $K^{-1}$  (see SI section 5 for determination), compared to 0.22 decades  $K^{-1}$  for posaconazole.

Previously published results can be interpreted to be consistent with RTS and this allows optimism that the method will be broadly useful for PVD glasses. GIWAXS data obtained at two deposition rates on Alq<sub>3</sub>,<sup>53</sup> a common OLED molecule, is consistent with RTS for molecular



packing with a shift factor of  $\sim 0.07$  decades  $K^{-1}$ . The molecular simulations of TPD deposition by Lyubimov et al.,<sup>46</sup> mentioned above, are also roughly consistent with RTS for molecular orientation. Finally, there is also evidence that RTS may be useful beyond organic glasses. Magnetic anisotropy measurements on amorphous Tb-Fe films show agreement with RTS and a model derived to describe these results is also consistent with RTS.<sup>12</sup> It will be of interest to determine if RTS can be extended to other inorganic glasses, including metallic glasses.

Due to its relevance to the field of organic electronics, it would be useful to test RTS for additional vapor-deposited organic glasses. Columnar liquid crystal systems are worthy of further investigation, due to their potential relevance in organic electronics<sup>54</sup> and the strong dependence of morphology upon substrate temperature.<sup>55</sup> Posaconazole is unique among non-liquid crystal molecules studied so far in that it anchors vertically at the surface, possibly due to its fluorine moieties that may segregate to the surface.<sup>33,37</sup> Among systems that do not form liquid crystal phases, the hole transport material TPD would be of interest as it has been extensively utilized in OLEDs. PVD glasses of TPD can show a considerable range of anisotropic structures and the equilibrium surface structure of TPD is different from that of posaconazole.<sup>13, 46, 56</sup>

## Conclusions

In summary, we find that the molecular orientation of vapor-deposited glasses of posaconazole, a system without known liquid crystal phases, obeys a Deposition Rate-Substrate Temperature superposition principle. The RTS can be understood through the surface equilibration mechanism that is responsible for the properties of vapor-deposited glasses. The orientational and translational order in posaconazole glasses prepared at low effective deposition rates supports the hypothesis that both the deposition rate and substrate temperature influence the depth to which the surface equilibrates during deposition. In addition to the utility of RTS to predict and control structure over a wide range of deposition conditions, RTS can be used to study and compare the dynamics of molecular motions at the surface of the glass. RTS has now been shown to describe a system without any liquid crystal phases, and could be further extended to systems with relevance to organic electronics.

## Supporting Information

The supporting information is available free of charge online.

Near-specular X-ray exposures, shift factor determinations, and fitting of surface and bulk relaxation times. (PDF)

### Acknowledgements

This research was primarily supported by NSF through the University of Wisconsin Materials Research Science and Engineering Center (Grant DMR-1720415). Use of the Stanford Synchrotron Radiation Lightsource, SLAC National Accelerator Laboratory, is supported by the US Department of Energy, Office of Science, Office of Basic Energy Sciences under Contract DE-AC02-76SF00515. We thank Dr. Jacob L. Thelen for useful discussion.

### References

1. Liu, Y.; Hata, S.; Wada, K.; Shimokohbe, A., Thermal, Mechanical and Electrical Properties of Pd-Based Thin-Film Metallic Glass. *Jpn. J. Appl. Phys.* **2001**, *40* (Part 1, No. 9A), 5382-5388.
2. Jain, H.; Vlcek, M., Glasses for lithography. *J. Non-Cryst. Solids* **2008**, *354* (12), 1401-1406.
3. Fortunato, E.; Barquinha, P.; Martins, R., Oxide Semiconductor Thin-Film Transistors: A Review of Recent Advances. *Adv. Mater.* **2012**, *24* (22), 2945-2986.
4. Ediger, M. D.; Forrest, J. A., Dynamics near Free Surfaces and the Glass Transition in Thin Polymer Films: A View to the Future. *Macromolecules* **2014**, *47* (2), 471-478.
5. Suga, H.; Seki, S., Thermodynamic investigation on glassy states of pure simple compounds. *J. Non-Cryst. Solids* **1974**, *16* (2), 171-194.
6. Yokoyama, D., Molecular orientation in small-molecule organic light-emitting diodes. *J. Mater. Chem.* **2011**, *21* (48), 19187-19202.
7. Mayr, C.; Taneda, M.; Adachi, C.; Brütting, W., Different orientation of the transition dipole moments of two similar Pt(II) complexes and their potential for high efficiency organic light-emitting diodes. *Org. Electron.* **2014**, *15* (11), 3031-3037.
8. Komino, T.; Tanaka, H.; Adachi, C., Selectively Controlled Orientational Order in Linear-Shaped Thermally Activated Delayed Fluorescent Dopants. *Chem. Mater.* **2014**, *26* (12), 3665-3671.
9. Ràfols-Ribé, J.; Will, P.-A.; Hänisch, C.; Gonzalez-Silveira, M.; Lenk, S.; Rodríguez-Viejo, J.; Reineke, S., High-performance organic light-emitting diodes comprising ultrastable glass layers. *Sci. Adv.* **2018**, *4* (5), eaar8332.
10. Snyder, C. R.; DeLongchamp, D. M., Glassy phases in organic semiconductors. *Curr. Opin. Solid St. M.* **2018**, *22* (2), 41-48.

11. Dharmapurikar, S. S.; Arulkashmir, A.; Das, C.; Muddellu, P.; Krishnamoorthy, K., Enhanced Hole Carrier Transport Due to Increased Intermolecular Contacts in Small Molecule Based Field Effect Transistors. *ACS Appl. Mater. Inter.* **2013**, *5* (15), 7086-7093.
12. Hellman, F., Surface-induced ordering: A model for vapor-deposition growth of amorphous materials. *Appl. Phys. Lett.* **1994**, *64* (15), 1947-1949.
13. Dalal, S. S.; Walters, D. M.; Lyubimov, I.; de Pablo, J. J.; Ediger, M. D., Tunable molecular orientation and elevated thermal stability of vapor-deposited organic semiconductors. *P. Natl. Acad. Sci. USA* **2015**, *112* (14), 4227.
14. Gujral, A.; Gómez, J.; Jiang, J.; Huang, C.; O'Hara, K. A.; Toney, M. F.; Chabinyk, M. L.; Yu, L.; Ediger, M. D., Highly Organized Smectic-like Packing in Vapor-Deposited Glasses of a Liquid Crystal. *Chem. Mater.* **2017**, *29* (2), 849-858.
15. Yu, H.-B.; Luo, Y.; Samwer, K., Ultrastable Metallic Glass. *Adv. Mater.* **2013**, *25* (41), 5904-5908.
16. Swallen, S. F.; Kearns, K. L.; Mapes, M. K.; Kim, Y. S.; McMahon, R. J.; Ediger, M. D.; Wu, T.; Yu, L.; Satija, S., Organic Glasses with Exceptional Thermodynamic and Kinetic Stability. *Science* **2007**, *315* (5810), 353-356.
17. Guo, Y.; Morozov, A.; Schneider, D.; Chung, J. W.; Zhang, C.; Waldmann, M.; Yao, N.; Fytas, G.; Arnold, C. B.; Priestley, R. D., Ultrastable nanostructured polymer glasses. *Nature Materials* **2012**, *11* (4), 337-343.
18. Kearns, K. L.; Swallen, S. F.; Ediger, M. D.; Wu, T.; Yu, L., Influence of substrate temperature on the stability of glasses prepared by vapor deposition. *J. Chem. Phys.* **2007**, *127* (15), 154702.
19. Rodríguez-Tinoco, C.; Gonzalez-Silveira, M.; Ràfols-Ribé, J.; Lopeandía, A. F.; Rodríguez-Viejo, J., Transformation kinetics of vapor-deposited thin film organic glasses: the role of stability and molecular packing anisotropy. *Phys. Chem. Chem. Phys.* **2015**, *17* (46), 31195-31201.
20. Dalal, S. S.; Sepúlveda, A.; Pribil, G. K.; Fakhraai, Z.; Ediger, M. D., Density and birefringence of a highly stable  $\alpha,\alpha,\beta$ - trisnaphthylbenzene glass. *Journal of Chemical Physics* **2012**, *136* (20), 204501.
21. Fakhraai, Z.; Still, T.; Fytas, G.; Ediger, M. D., Structural Variations of an Organic Glassformer Vapor-Deposited onto a Temperature Gradient Stage. *J. Phys. Chem. Lett.* **2011**, *2* (5), 423-427.
22. Swallen, S. F.; Kearns, K. L.; Mapes, M. K.; Kim, Y. S.; McMahon, R. J.; Ediger, M. D.; Wu, T.; Yu, L.; Satija, S., Organic Glasses with Exceptional Thermodynamic and Kinetic Stability. *Science* **2007**, *315* (5810), 353.
23. Yu, L., Surface mobility of molecular glasses and its importance in physical stability. *Adv. Drug. Deliver. Rev.* **2016**, *100*, 3-9.
24. Harrowell, P., Orientationally ordered glasses via controlled deposition. *P. Natl. Acad. Sci. USA* **2019**, *116* (43), 21341.
25. Tarnacka, M.; Adrjanowicz, K.; Kaminska, E.; Kaminski, K.; Grzybowska, K.; Kolodziejczyk, K.; Wlodarczyk, P.; Hawelek, L.; Garbacz, G.; Kocot, A.; Paluch, M., Molecular dynamics of itraconazole at ambient and high pressure. *Phys. Chem. Chem. Phys.* **2013**, *15* (47), 20742-20752.
26. Teerakapibal, R.; Huang, C.; Gujral, A.; Ediger, M. D.; Yu, L., Organic Glasses with Tunable Liquid-Crystalline Order. *Phys. Rev. Lett.* **2018**, *120* (5), 055502.

27. Bishop, C.; Gujral, A.; Toney, M. F.; Yu, L.; Ediger, M. D., Vapor-Deposited Glass Structure Determined by Deposition Rate–Substrate Temperature Superposition Principle. *J. Phys. Chem. Lett.* **2019**, *10* (13), 3536-3542.
28. Laventure, A.; Gujral, A.; Lebel, O.; Pellerin, C.; Ediger, M. D., Influence of Hydrogen Bonding on the Kinetic Stability of Vapor-Deposited Glasses of Triazine Derivatives. *J. Phys. Chem. B* **2017**, *121* (10), 2350-2358.
29. Chen, Y.; Zhu, M.; Laventure, A.; Lebel, O.; Ediger, M. D.; Yu, L., Influence of Hydrogen Bonding on the Surface Diffusion of Molecular Glasses: Comparison of Three Triazines. *J. Phys. Chem. B* **2017**, *121* (29), 7221-7227.
30. Zhang, W.; Brian, C. W.; Yu, L., Fast Surface Diffusion of Amorphous o-Terphenyl and Its Competition with Viscous Flow in Surface Evolution. *J. Phys. Chem. B* **2015**, *119* (15), 5071-5078.
31. Samanta, S.; Huang, G.; Gao, G.; Zhang, Y.; Zhang, A.; Wolf, S.; Woods, C. N.; Jin, Y.; Walsh, P. J.; Fakhraai, Z., Exploring the Importance of Surface Diffusion in Stability of Vapor-Deposited Organic Glasses. *J. Phys. Chem. B* **2019**, *123* (18), 4108-4117.
32. Chen, Y.; Chen, Z.; Tylinski, M.; Ediger, M. D.; Yu, L., Effect of molecular size and hydrogen bonding on three surface-facilitated processes in molecular glasses: Surface diffusion, surface crystal growth, and formation of stable glasses by vapor deposition. *J. Chem. Phys.* **2019**, *150* (2), 024502.
33. Moore, A. R.; Huang, G.; Wolf, S.; Walsh, P. J.; Fakhraai, Z.; Riggleman, R. A., Effects of microstructure formation on the stability of vapor-deposited glasses. *P. Natl. Acad. Sci. USA* **2019**, *116* (13), 5937.
34. Dannhauser, W.; Child, W. C.; Ferry, J. D., Dynamic Mechanical Properties of Poly-n-octyl methacrylate. *J. Colloid Interface Sci.* **1958**, *13*, 103-113.
35. Richert, R.; Duvvuri, K.; Duong, L. T., Dynamics of glass-forming liquids. VII. Dielectric relaxation of supercooled tris-naphthylbenzene, squalane, and decahydroisoquinoline. *J. Chem. Phys.* **2003**, *118*, 1828-1836.
36. Roland, C. M.; Casalini, R.; Paluch, M., Isochronal temperature–pressure superpositioning of the  $\alpha$ -relaxation in type-A glass formers. *Chem. Phys. Lett.* **2003**, *367* (3), 259-264.
37. Bishop, C.; Thelen, J. L.; Gann, E.; Toney, M. F.; Yu, L.; DeLongchamp, D. M.; Ediger, M. D., Vapor deposition of a nonmesogen prepares highly structured organic glasses. *P. Natl. Acad. Sci. USA* **2019**, *116* (43), 21421.
38. Gómez, J.; Gujral, A.; Huang, C.; Bishop, C.; Yu, L.; Ediger, M. D., Nematic-like stable glasses without equilibrium liquid crystal phases. *J. Chem. Phys.* **2017**, *146* (5), 054503.
39. Baker, J. L.; Jimison, L. H.; Mannsfeld, S.; Volkman, S.; Yin, S.; Subramanian, V.; Salleo, A.; Alivisatos, A. P.; Toney, M. F., Quantification of Thin Film Crystallographic Orientation Using X-ray Diffraction with an Area Detector. *Langmuir* **2010**, *26* (11), 9146-9151.
40. Oosterhout, S. D.; Savikhin, V.; Zhang, J.; Zhang, Y.; Burgers, M. A.; Marder, S. R.; Bazan, G. C.; Toney, M. F., Mixing Behavior in Small Molecule:Fullerene Organic Photovoltaics. *Chem. Mater.* **2017**, *29* (7), 3062-3069.
41. Zhang, F.; Ilavsky, J.; Long, G. G.; Quintana, J. P. G.; Allen, A. J.; Jemian, P. R., Glassy Carbon as an Absolute Intensity Calibration Standard for Small-Angle Scattering. *Metall. Mater. Trans. A* **2010**, *41* (5), 1151-1158.
42. Ilavsky, J., Nika: software for two-dimensional data reduction. *J. Appl. Crystallogr.* **2012**, *45*, 324-328.

43. Mapesa, E. U.; Tarnacka, M.; Kamińska, E.; Adrjanowicz, K.; Dulski, M.; Kossack, W.; Tress, M.; Kipnusu, W. K.; Kamiński, K.; Kremer, F., Molecular dynamics of itraconazole confined in thin supported layers. *RSC Advances* **2014**, *4* (54), 28432-28438.
44. Adrjanowicz, K.; Kaminski, K.; Włodarczyk, P.; Grzybowska, K.; Tarnacka, M.; Zakowiecki, D.; Garbacz, G.; Paluch, M.; Jurga, S., Molecular Dynamics of the Supercooled Pharmaceutical Agent Posaconazole Studied via Differential Scanning Calorimetry and Dielectric and Mechanical Spectroscopies. *Mol. Pharmaceut.* **2013**, *10* (10), 3934-3945.
45. Gómez, J.; Jiang, J.; Gujral, A.; Huang, C.; Yu, L.; Ediger, M. D., Vapor deposition of a smectic liquid crystal: highly anisotropic, homogeneous glasses with tunable molecular orientation. *Soft Matter* **2016**, *12* (11), 2942-2947.
46. Lyubimov, I.; Antony, L.; Walters, D. M.; Rodney, D.; Ediger, M. D.; de Pablo, J. J., Orientational anisotropy in simulated vapor-deposited molecular glasses. *J. Chem. Phys.* **2015**, *143* (9), 094502.
47. Zhang, W.; Yu, L., Surface Diffusion of Polymer Glasses. *Macromolecules* **2016**, *49* (2), 731-735.
48. Liu, F.; Brady, M. A.; Wang, C., Resonant soft X-ray scattering for polymer materials. *Eur. Polym. J.* **2016**, *81*, 555-568.
49. Haji-Akbari, A.; Debenedetti, P. G., Thermodynamic and kinetic anisotropies in octane thin films. *J. Chem. Phys.* **2015**, *143* (21), 214501.
50. Kim, H.; Cang, Y.; Kang, E.; Graczykowski, B.; Secchi, M.; Montagna, M.; Priestley, R. D.; Furst, E. M.; Fytas, G., Direct observation of polymer surface mobility via nanoparticle vibrations. *Nat. Comm.* **2018**, *9* (1), 2918.
51. Paeng, K.; Swallen, S. F.; Ediger, M. D., Direct Measurement of Molecular Motion in Freestanding Polystyrene Thin Films. *J. Am. Chem. Soc.* **2011**, *133* (22), 8444-8447.
52. Liu, Y.; Russell, T. P.; Samant, M. G.; Stöhr, J.; Brown, H. R.; Cossy-Favre, A.; Diaz, J., Surface Relaxations in Polymers. *Macromolecules* **1997**, *30* (25), 7768-7771.
53. Bagchi, K.; Jackson, N. E.; Gujral, A.; Huang, C.; Toney, M. F.; Yu, L.; de Pablo, J. J.; Ediger, M. D., Origin of Anisotropic Molecular Packing in Vapor-Deposited Alq3 Glasses. *J. Phys. Chem. Lett.* **2019**, *10* (2), 164-170.
54. Wöhrle, T.; Wurzbach, I.; Kirres, J.; Kostidou, A.; Kapernaum, N.; Litterscheidt, J.; Haenle, J. C.; Staffeld, P.; Baro, A.; Giesselmann, F.; Laschat, S., Discotic Liquid Crystals. *Chem. Rev.* **2016**, *116* (3), 1139-1241.
55. Gujral, A.; Gómez, J.; Ruan, S.; Toney, M. F.; Bock, H.; Yu, L.; Ediger, M. D., Vapor-Deposited Glasses with Long-Range Columnar Liquid Crystalline Order. *Chem. Mater.* **2017**, *29* (21), 9110-9119.
56. Ràfols-Ribé, J.; Dettori, R.; Ferrando-Villalba, P.; Gonzalez-Silveira, M.; Abad, L.; Lopeandía, A. F.; Colombo, L.; Rodríguez-Viejo, J., Evidence of thermal transport anisotropy in stable glasses of vapor deposited organic molecules. *Phys. Rev. Mater.* **2018**, *2* (3), 035603.

TOC Image

